



A numerical study on the low-velocity impact response of hybrid composite materials

Uzay Gezer*¹, Bünyamin Demir ¹, Yusuf Kepir ¹, Alper Gunoz ¹, Memduh Kara ¹

¹Mersin University, Department of Mechanical Engineering, Türkiye

Keywords

Composites
Glass Fiber
Aramid Fiber
Low-velocity Impact
LS-DYNA

Research Article

DOI: 10.31127/tuje.1191785

Received: 19.10.2022

Revised: 06.11.2022

Accepted: 19.11.2022

Published: 27.02.2023



Abstract

Composite materials are advanced engineering materials with superior properties to traditional materials. One of the most important disadvantages is the high cost of composite materials. Therefore, producing composite materials from the first to the last stage is a very important process. Homogenization is the most important parameter in production since composites contain more than one material type in their structure. In addition, composite structures are sensitive materials against low-velocity impacts. In this study, the effect of reinforcement material combination and stacking sequence on mechanical properties used in the production of composite materials was investigated by low-velocity impact simulations using LS-DYNA software. The mass of the 12 mm diameter spherical impactor used in the analyzes was determined as 10 kg and low-velocity impact tests were applied at 20 J, 30 J and 40 J energy levels. The composite samples were modeled with 180x100mm dimensions and the contact between the impactor and the sample was made from the center of the composite structure. Numerical analyzes were performed using the Tsai-Wu damage criterion in the LS-DYNA software, and material properties were defined using the "Mat_Enhanced_Composite_Damage (MAT 055)" material card.

1. Introduction

Nowadays, instead of traditional materials such as metal, wood, polymer, composite materials that combine the excellent properties of their constituent components are used in many industries. Since the materials used in industrial production are desired to have superior properties, the need for new material types is increasing daily [1]. In line with this need, research and development studies have focused on the production of new composite materials with superior properties by changing material combinations.

While epoxy resin is generally used as matrix material in the production of fiber reinforced composite materials, glass fiber, carbon fiber, basalt fiber and aramid fiber are used extensively as reinforcement materials. In addition, hybrid composites that these fibers are used together has been increasing rapidly in recent years. The most important reasons for the widespread use of fiber-reinforced polymer composites are their high strength and modulus of elasticity.

Fiber reinforced composites can also be produced as hybrids using more than one fiber type. Hybrid composites can have better mechanical properties when comparing pure fiber composites. In hybrid composite materials, the stacking sequence can positively or negatively affect the mechanical behavior of the composite structures. For this reason, it is crucial to subject different stacking sequences hybrid composite samples to mechanical tests. In some scientific research that includes composite materials, the stacking sequence's effect on mechanical strength has been investigated [2-5].

Reinforcement materials such as glass, carbon and aramid fiber are widely used as reinforcement components in composite materials. The tensile strength of glass fibers is considerably higher than polymers. They also have a high strength-to-weight ratio [6,7]. Aramid fibers have superior characteristics such as high strength, high modulus of elasticity, high temperature resistance, high chemical corrosion resistance and high shear strength [8-11].

* Corresponding Author

* (uzaygezer@mersin.edu.tr) ORCID ID 0000-0003-3088-7610
(bd@mersin.edu.tr) ORCID ID 0000-0002-6405-4724
(ykepir@mersin.edu.tr) ORCID ID 0000-0002-3536-3931
(alpergunoz@mersin.edu.tr) ORCID ID 0000-0001-7978-6306
(memduhkara@mersin.edu.tr) ORCID ID 0000-0002-5201-5453

Cite this article

Gezer, U., Demir, B., Kepir, Y., Gunoz, A., & Kara, M. (2023). A numerical study on the low-velocity impact response of hybrid composite materials. Turkish Journal of Engineering, 7(4), 314-321

In engineering applications, besides experimental studies, there are many studies in which results are obtained with numerical analysis without the need for experimentation [12-16]. Tests are carried out to determine the mechanical strength of composite materials that cause costs in terms of both material and labor. Today, these tests can be done by physically, also can be done by numerical analysis in computers. ANSYS and LS-DYNA software are widely used in the numerical analysis of composite materials. According to the tests to be applied, the properties of the samples, which are modeled in three dimensions in the computer environment, can be defined on the material cards which in the software interface and numerical analyzes can be made. Thus these numerical analyzes, the mechanical behavior of the material planned to be produced can be tested virtually. Eventually, the numerical analysis can save labor and material costs.

Song [17] examined the tensile and bending strengths of layered composites prepared by carbon/glass and carbon/aramid fiber hybridization. Composite samples, which were formed by using six different layer numbers and stacking sequences, were produced by vacuum assisted resin transfer method. As a result of the study, it was concluded that both carbon/glass and carbon/aramid hybrid composites have much better tensile and flexural strengths of samples with carbon in the interior compared to samples with other stacking sequences.

Jaroslaw et al. [18] produced composite samples based on aluminum alloy and glass or carbon fiber reinforced laminated polymer composites and investigated their low-velocity impact behavior. They analyzed the effect of fiber stacking sequence angles by interpreting the damage and impact responses. As a result of the study, they observed that while plastic deformation creation, delamination initiation and progression were seen in samples containing glass fiber, collapse (penetration) and puncture (perforation) occurred in samples that containing carbon fiber.

Wagih et al. [19], investigated the low-velocity impact responses of carbon fiber and aramid fiber reinforced hybrid composites at different energy levels. Three-point bending tests were applied to the impact damaged samples and compared with the flexural strength of the undamaged samples. They observed that in the samples placed aramid fiber between the carbon fiber layers, no damage occurred in the lowest carbon layer as a result of low-velocity impact. They concluded that aramid reinforcement significantly increased the strength of the samples compared to pure carbon fiber reinforced and pure glass fiber reinforced composites.

Gemi et al. [20] applied low-velocity impact tests at 4 different velocities to 6 layers of glass fiber reinforced ring composites produced in 3 different diameters. It was observed that the energy absorption ability decreased with the increase of the impact velocity. As a result of the study, it was concluded that as the diameter of the samples increased, the maximum contact force and the amount of absorbed energy decreased [20].

Rezasefat et al. [21], produced 8 layers of aramid fiber and glass fiber hybrid composites and applied a low-velocity impact test. They investigated the effect of

hybridization and stacking sequence on impact resistance in samples exposed to impact at 19 J, 37 J and 72 J energy levels. As a result, it was seen that the resistance to impact increased up to the energy level of 49.5 J with hybridization, and at higher energy levels, the pure glass fiber reinforced composite performed better.

Uyaner et al. [22] investigated the impact response of 18-layer E-glass fiber reinforced composites with different sized experimentally and numerically. Numerical analyzes were performed with the MAT 055 material model using the LS-DYNA software. According to the results of the numerical and experimental, it was determined that the size of the composite materials remarkably affects the impact behavior of the materials.

Mesh density is a significant parameter in studies that includes finite element analysis. According to the mesh number determined in the analysis, the results may vary up to the optimum mesh number value, but there is no visible change in the results obtained after the optimum mesh number is reached [22]. In this work, the contact force values were determined at an element size of 2 mm, corresponding to the number of elements in one plate being 4500. Also, the impactor was created with 12096 elements.

Composite materials can be exposed to low-velocity impacts at different energy levels during their lifetime. These impacts result in different types of damages in composite structures. The researchers applied impact simulations at different energy levels to the materials which is modeled three-dimensionally in the computer environment and aimed to create predictions against impacts that could be encountered in real life with the data they obtained. In these studies, in the literature, generally 20 J and 30 J energy levels were used [23,24].

In this study, 12-layer glass fiber/epoxy, aramid fiber/epoxy composites and glass fiber/aramid fiber/epoxy hybrid composites were modeled with LS-DYNA software and the low-velocity impact test was simulated in a virtual environment. Impact energies were determined as 20 J, 30 J and 40 J in analyzes which performed on 6 different composite models. The stacking sequences of the layers forming the composites are common to all samples and the form of stacking sequences angles [0,90]₆. This study aims to predict the impact response of composite materials, which are very difficult and costly to manufacture, with a preliminary evaluation made in the computer environment.

2. Method

In this study, six different composite material designs were first carried out. Glass fiber and aramid fiber were chosen as reinforcement material and epoxy resin as matrix material. Composite structures modeled in Figure 1 are given schematically. The designed composite structures are pure aramid epoxy [A]₁₂, pure glass epoxy [C]₁₂, hybrid1 [AC]₆, hybrid2 [CA]₆, functional1 [AAAAAACCCCCC] and functional2 [CCCCCAAAAAA]. All samples are designed to be 180 × 100mm in size with 12 layers. Low-velocity impact tests were applied to the designed samples at 20 J, 30 J and 40 J energy levels. During the impact tests, the samples were modeled as free (180 mm) on both sides and embedded

(100 mm) on both sides. LS-DYNA software, which is widely used in the literature, was preferred for performing low-velocity impact tests.

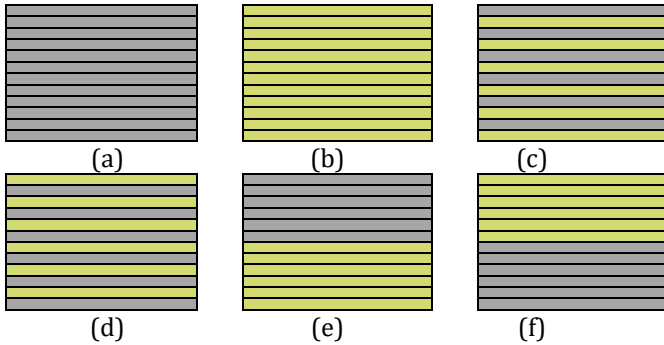


Figure 1. Designed 12-layer composite samples (a) pure glass fiber, (b) pure aramid fiber, (c) hybrid1, (d) hybrid2, (e) functional1 and (f) functional2

In order to define the layer properties of composite samples;

MAT055 (MAT_ENHANCED_COMPOSITE_DAMAGE) material card is used. The MAT 055 material card uses the Tsai-Wu damage criterion in numerical analysis, and the formula technique is given in Equation 1-3.

Tensile damage in fiber direction;

$$\left(\frac{\sigma_{11}}{X_T}\right)^2 + \beta \left(\frac{\sigma_{12}}{S_C}\right)^2 - 1 \begin{cases} \geq 0 & \text{failed} \\ \leq 0 & \text{elastic} \end{cases} \quad (1)$$

Compression damage in the fiber direction;

$$\left(\frac{\sigma_{11}}{X_C}\right)^2 - 1 \begin{cases} \geq 0 & \text{failed} \\ \leq 0 & \text{elastic} \end{cases} \quad (2)$$

Tensile and compression damages in the transverse fiber direction;

$$\left(\frac{\sigma_{22}}{Y_C Y_T}\right)^2 + \left(\frac{\sigma_{12}}{S_C}\right)^2 + \left(\frac{\sigma_{22}(Y_C - Y_T)}{Y_C Y_T}\right) - 1 \begin{cases} \geq 0 & \text{failed} \\ \leq 0 & \text{elastic} \end{cases} \quad (3)$$

calculated using the formulas. The subscript “1” denotes the fiber array direction, and the “2” denotes the transverse fiber direction (the normal of the fiber). σ_{11} is the normal stress in the fiber direction, σ_{12} is the in-plane shear stress, σ_{22} is the transverse normal stress in the fiber direction, and β is the weight factor in the shear stress. S_C corresponds to interlayer shear strength, X_C longitudinal compression strength, X_T longitudinal tensile strength, Y_T cross-sectional tensile strength and Y_C cross-sectional compression strength values.

Composite samples were modeled as 12 different layers, and aramid/epoxy and glass/epoxy layer properties were defined for each layer using the Part Composite material card. The layers are connected to each other using with the Contact Automatic_One_Way_Surface_To_Surface_Tiebreak material card. In accordance with the literature, the glass/epoxy layer thickness is 0.2125 mm and the aramid/epoxy layer thickness is 0.3875 mm [22]. The material properties of aramid/epoxy layers are given in Table 1, and the material properties of glass/epoxy layers are given in Table 2.

Table 1. Material properties of aramid/epoxy ply [25]

LS-DYNA Flag	Value	Unit
E ₁₁	40300	MPa
E ₂₂	10300	MPa
G ₁₂	2500	MPa
V ₁₂	0.23	-
X _T	743	MPa
X _C	249.6	MPa
Y _T	59.4	MPa
Y _C	87.6	MPa
S _C	34.5	MPa
DFAILT	0.0184	-
DFAILC	0.0062	-
DFAILM	0.0058	-
DFAILS	0.0138	-

Table 2. Material properties of glass fiber/epoxy ply [22]

LS-DYNA Flag	Value	Unit
E ₁₁	42000	MPa
E ₂₂	9500	MPa
G ₁₂	3500	MPa
V ₁₂	0.34	-
X _T	690	MPa
X _C	300	MPa
Y _T	66	MPa
Y _C	147	MPa
S _C	56	MPa
DFAILT	0.0164	-
DFAILC	0.0071	-
DFAILM	0.0069	-
DFAILS	0.0160	-

The impactor properties used in the numerical analysis are given in Table 3. Impact material properties, modeled as solid spherical and 12 mm in diameter, were defined using the MAT_020 Rigid material card. The MAT_020 material card has been used in many low-velocity impact studies in the scientific studies [26]. The impactor was defined as having a mass of 10 kg and its density was determined as 1.112885 kg/m³. The connection between the impactor and the composite sample was established with the CONTACT_AUTOMATIC_NODES_TO_SURFACE material card and numerical analysis was performed [27].

Table 3. Material properties of impactor [23]

Material	Density, ρ	Modulus of elasticity, E	Poisson's ratio
Steel	1.112885 kg/m ³	207000 MPa	0.3

3. Results

In low-velocity impact tests using LS-DYNA software, 20 J, 30 J and 40 J impact energy levels were preferred. Low-velocity impact tests with the specified properties were applied to the modeled samples by making 6 different combinations, force-time and force-displacement graphs were created.

In Figure 2a force-time and Figure 2b force-displacement graphs of 12-layer glass fiber composite samples at different energy levels are given.

Figure 3 shows (a) force-time and (b) force-displacement histories of 12-layer aramid fiber composite sample at different energy levels.

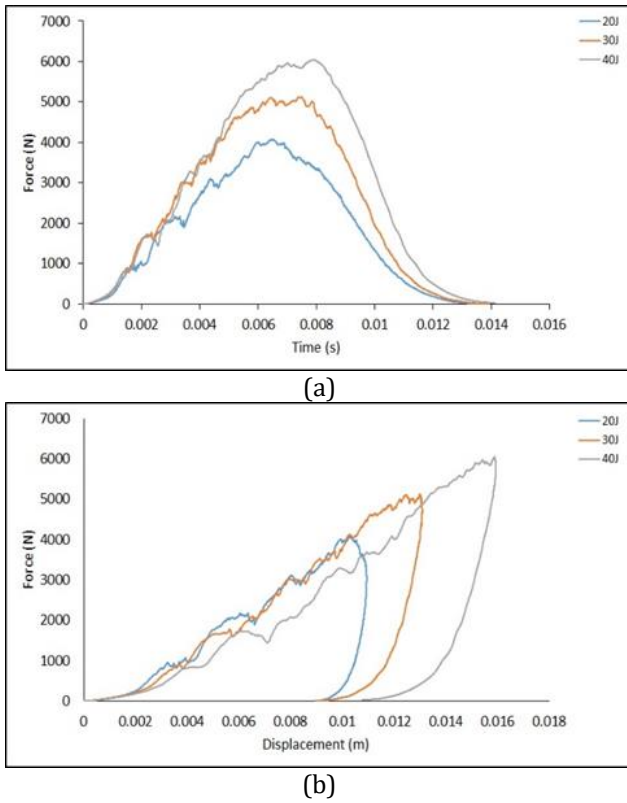


Figure 2. The graphs of (a) force-time and (b) force-displacement for 12-layer glass fiber composite sample at different energy levels

When the force-time histories given in Figure 2a are examined, it is seen that the contact force increases rapidly as the impactor contacts the sample and starts to decrease after reaching a certain value. Since the impactor rebound from the sample surface, the contact force value decreased to 0 at all energy levels. It is seen that the force-time changes are in the form of a bell-shaped curve for all energy levels. Vibrations occurring especially in the part where the force increases, indicate that the composite samples are damaged [28]. As the impact energy level increases, the maximum contact force value also increases. In Figure 2b, the force-displacement changes for different energy levels are given together. The slope in the increasing part of the force-displacement change is called bending rigidity in the scientific research due to the resistance of the sample against the impact load [22]. While the bending rigidity value was nearly same at 20 J and 30 J energy levels, it decreased at 40 J energy level. This indicates that the resistance of the glass fiber/epoxy composite sample decreases somewhat with the increase in the energy level. As the impact energy increases, sample's displacement increases. The area under the force-displacement curve gives the amount of energy absorbed by the material during the impact. It is clearly seen from the graphs that the amount of energy absorbed increases with the increase of the impact energy.

When the force-time changes given in Figure 3a are examined, it is seen that the force increases rapidly with the contact of the impactor to the sample, similar to the glass fiber/epoxy sample, and decreases to 0 after reaching a certain value. The highest contact force values obtained for the same energy levels were higher in

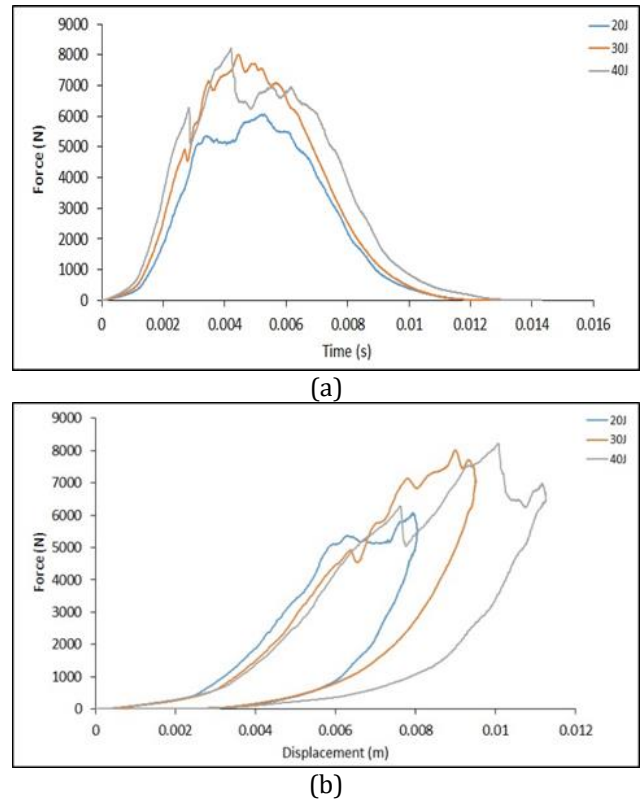


Figure 3. The graphs of (a) force-time and (b) force-displacement for 12-layer aramid fiber composite sample at different energy levels

aramid fiber/epoxy samples. The most important reason for this is that aramid fiber behaves more rigidly than glass fiber. As the stiffness of the specimen increased, the maximum contact force value also increased. Figure 3b shows the force-displacement changes of the aramid fiber/epoxy composite sample for different energy levels. When the graph is examined, it is seen that the bending rigidity value for the 20 J energy level is higher than the others. The bending rigidity values at 30 J and 40 J energy levels were nearly same. For the same energy level, it is seen that the largest displacement value in the samples is lower than the glass fiber/epoxy composite samples.

In Figure 4, 12-layer hybrid1 and in Figure 5, 12 layer hybrid2 glass and aramid fiber reinforced composite samples' (a) force-time and (b) force-displacement graphs are given.

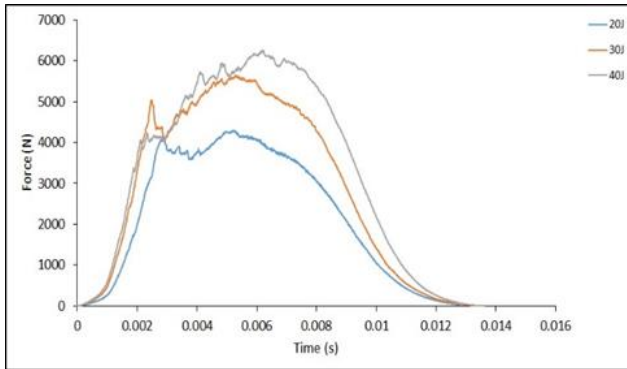
When the force-time changes given for the hybrid1 sample in Figure 4a and for the hybrid2 sample in Figure 5a are examined, they are characteristically similar to the graphs obtained from pure glass and pure aramid composite samples. The highest contact force values obtained from hybrid1 and hybrid2 composite samples were found to be higher than pure glass sample and lower than pure aramid sample for the same energy level. When the hybrid1 and hybrid2 samples were evaluated within themselves, it was seen that the highest contact force value obtained from the hybrid2 sample was higher for the 20 J energy level. The maximum contact force values were nearly the same for 30 J and 40 J energy levels. The impacted surface in the hybrid2 sample is the aramid surface and has a higher stiffness value. This resulted in a higher contact force for the 20 J energy level.

Since the damage to the samples will increase at other energy levels, the impact response was similar.

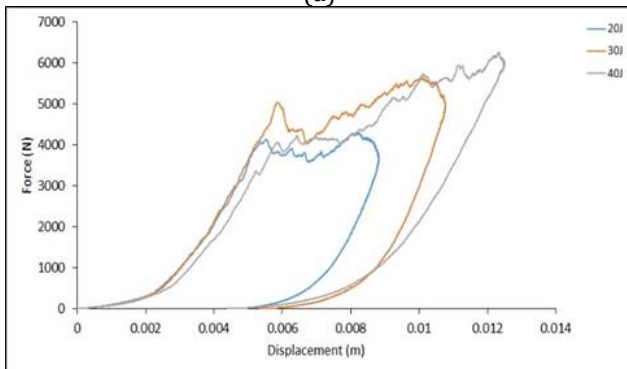
Force-displacement graphs at different energy levels are given for the hybrid1 sample in Figure 4b, and for the hybrid2 sample in Figure 5b. When the graphs are examined, the bending stiffness values of the hybrid1 sample impacted from the glass surface were nearly the same for 20 J and 30 J energy levels, but decreased at 40 J energy level. This variation is similar to a pure glass sample. On the other hand, bending rigidity values at 30 J and 40 J energy levels were nearly same in hybrid2 sample, which was impacted by the aramid surface, while

bending stiffness was higher at 20 J energy level. This change was similar to the force-displacement changes obtained from the pure aramid sample. When the maximum displacement values for the same energy level are examined, it is seen that nearly same displacement values are reached in hybrid1 and hybrid2 samples.

In Figure 6a and Figure 7a force-time, Figure 6b and Figure 7b force-displacement graphs of 12-layer functional1 and 12-layer functional2 glass and aramid fiber reinforced composite samples are given at different energy levels.



(a)

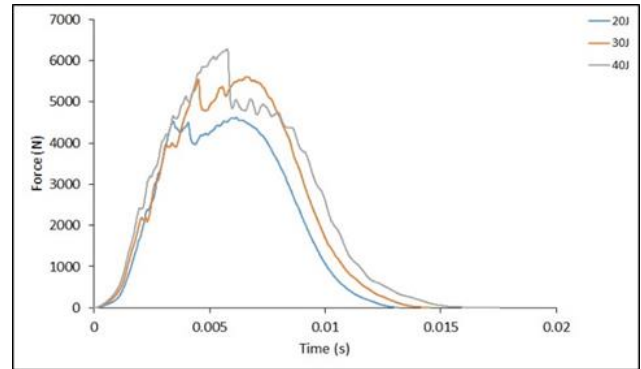


(b)

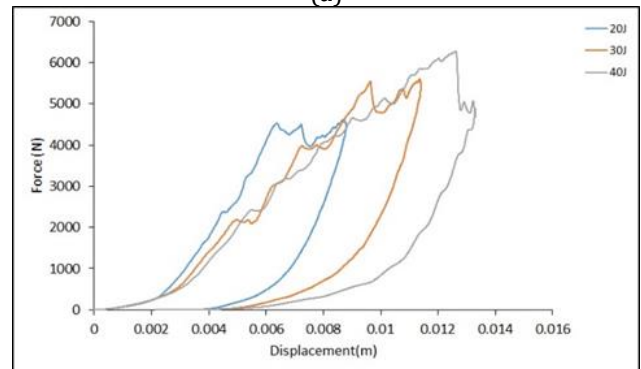
Figure 4. The graphs of (a) force-time and (b) force-displacement for 12-layer hybrid1 glass and aramid fiber reinforced composite sample at different energy levels

When the force-time changes given for the functional1 sample in Figure 6a and for the functional2 sample in Figure 7a are examined, the maximum contact force values obtained from the same energy levels were lower than the previous samples. When the functional1 and functional2 composite samples were evaluated within themselves, lower force values were obtained for the same energy level than the functional1 sample. Obtaining lower force values by producing the samples functionally indicates that the samples' stiffness has decreased. Otherwise, raw material of the impacted surface for functional samples is extremely important in impact responses.

Force-displacement graphs at different energy levels are given for the functional1 sample in Figure 6b and for the functional2 sample in Figure 7b. For the same energy levels, higher displacement values were obtained from the functional2 sample compared to the functional1 sample. When the bending rigidity values in force-displacement changes are examined, different values



(a)



(b)

Figure 5. The graphs of (a) force-time and (b) force-displacement for 12-layer hybrid2 glass and aramid fiber reinforced composite sample at different energy levels

occur at different energy levels in the functional1 sample, while nearly same bending rigidity values are obtained in the functional2 sample.

4. Conclusion

Composite materials are frequently used in aviation, space, automotive and defense industry sectors due to their superior properties such as high strength/weight ratio, high wear and corrosion resistance. The most disadvantageous features of composite materials are their sensitivity to impact loading and their high cost. For this reason, predicting the damages that will occur with impact load in composite materials and designing them accordingly will make a significant contribution to reducing the cost. In this study, the low-velocity impact response of 180x100mm glass, aramid and hybrid composite materials at 20 J, 30 J and 40 J energy levels was investigated using LS-Dyna software. The results obtained from the study are presented below;

- When the force-time histories of all test samples at different energy levels were examined, it was determined that the maximum contact force increased with the increase of the impact energy. It was observed that the oscillations indicating damage also increased with the increase of the impact energy.
- In the force-displacement curves of the 12-layer glass fiber composite sample, the bending rigidity value was nearly same for 20 J and 30 J, but decreased slightly at the 40 J energy level.
- In the force-displacement curves of the 12-layer aramid fiber composite sample, the bending rigidity value was found to be higher at 20 J energy levels than the other energy levels, and nearly same at 30 J and 40 J energy levels.
- In the force-displacement curves of the hybrid1 sample, it was observed that the bending rigidity values at 20 J and 30 J energy levels were nearly same,

but decreased at 40 J energy level. On the other hand, for the hybrid 2 composite sample, while the bending rigidity value was nearly same at 30 J and 40 J energy levels, but it was higher at 20 J energy level.

- Force-displacement curves of the functional1 sample show that different bending rigidities occur at different energy levels; The graphs of the functional 2 sample show that nearly same bending rigidities occur at different energy levels.
- The area under the force-displacement curves gives the amount of absorbed energy by the sample during the impact. For all test samples, as the impact energy increased, the amount of absorbed energy also increased.
- Since this study examines the low-velocity impact responses of aramid and glass fiber reinforced composites at different energy levels, it will lead to future studies on this subject.

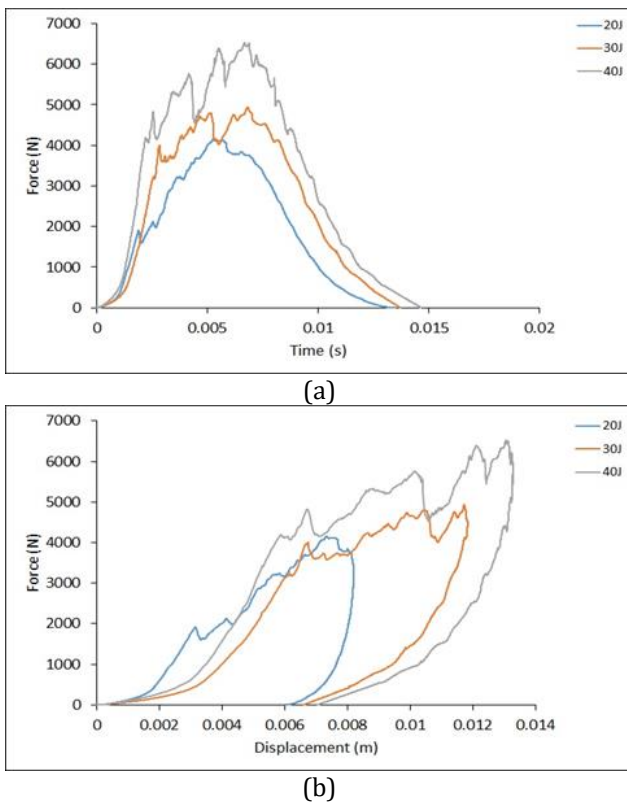


Figure 6. The graphs of (a) force-time and (b) force-displacement for 12-layer functionally graded glass and aramid fiber reinforced functional1 composite sample at different energy levels

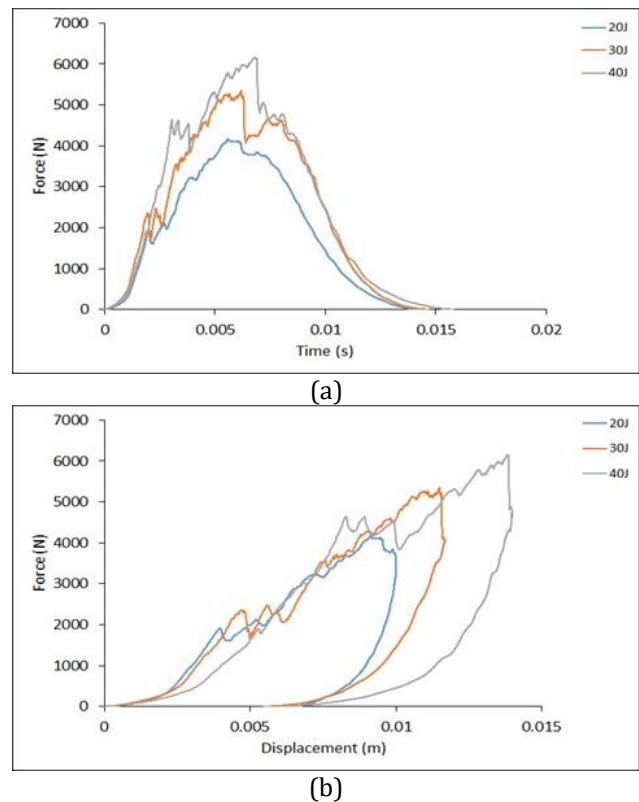


Figure 7. The graphs of (a) force-time and (b) force-displacement for 12-layer functionally graded glass and aramid fiber reinforced functional2 composite sample at different energy levels

Acknowledgement

We would like to thank Erzurum Atatürk University for the LS-DYNA software which is used in the numerical analysis in this study.

Author contributions

Uzay Gezer: Investigation, Methodology, Software, Writing-Original draft preparation. **Bünyamin Demir:** Conceptualization, Methodology, Data curation, Validation. **Yusuf Kepir:** Investigation, Software,

Writing-Reviewing and Editing. **Alper Günöz:** Software, Visualization and Editing. **Memduh Kara:** Conceptualization, Visualization, Writing-Reviewing and Editing.

Conflicts of interest

The authors declare no conflicts of interest.

References

1. Naqvi, S. R., Prabhakara, H. M., Bramer, E. A., Dierkes, W., Akkerman, R., & Brem, G. (2018). A critical review on recycling of end-of-life carbon fibre/glass fibre reinforced composites waste using pyrolysis towards a circular economy. *Resources, conservation and recycling*, 136, 118-129.
2. Lin, S., & Waas, A. M. (2021). The effect of stacking sequence on the LVI damage of laminated composites; experiments and analysis. *Composites Part A: Applied Science and Manufacturing*, 145, 106377.
3. Kazemi, M. E., Shanmugam, L., Dadashi, A., Shakouri, M., Lu, D., Du, Z., ... & Yang, J. (2021). Investigating the roles of fiber, resin, and stacking sequence on the low-velocity impact response of novel hybrid thermoplastic composites. *Composites Part B: Engineering*, 207, 108554.
4. Supian, A. B. M., Sapuan, S. M., Jawaid, M., Zuhri, M. Y. M., Ilyas, R. A., & Syamsir, A. (2022). Crashworthiness response of filament wound kenaf/glass fibre-reinforced epoxy composite tubes with influence of stacking sequence under intermediate-velocity impact load. *Fibers and Polymers*, 23(1), 222-233.
5. Garouge, S. E., Tarfaoui, M., Hassoon, O. H., Minor, H. E., & Bendarma, A. (2022). Effect of stacking sequence on the mechanical performance of the composite structure under slamming impact. *Materials Today: Proceedings*, 52, 29-39.
6. Goh, G. D., Dikshit, V., Nagalingam, A. P., Goh, G. L., Agarwala, S., Sing, S. L., ... & Yeong, W. Y. (2018). Characterization of mechanical properties and fracture mode of additively manufactured carbon fiber and glass fiber reinforced thermoplastics. *Materials & Design*, 137, 79-89.
7. Günöz, A., Kepir, Y. & Kara, M. (2022). The investigation of hardness and density properties of GFRP composite pipes under seawater conditions. *Turkish Journal of Engineering*, 6 (1), 34-39 .
8. Yang, G., Park, M., & Park, S. J. (2019). Recent progresses of fabrication and characterization of fibers-reinforced composites: A review. *Composites Communications*, 14, 34-42.
9. Lertwassana, W., Parnklang, T., Mora, P., Jubsilp, C., & Rimdusit, S. (2019). High performance aramid pulp/carbon fiber-reinforced polybenzoxazine composites as friction materials. *Composites Part B: Engineering*, 177, 107280.
10. Qi, G., Zhang, B., Du, S., & Yu, Y. (2017). Estimation of aramid fiber/epoxy interfacial properties by fiber bundle tests and multiscale modeling considering the fiber skin/core structure. *Composite Structures*, 167, 1-10.
11. Raphael, N., Namratha, K., Chandrashekar, B. N., Sadasivuni, K. K., Ponnamma, D., Smitha, A. S., ... & Byrappa, K. J. P. I. C. G. (2018). Surface modification and grafting of carbon fibers: A route to better interface. *Progress in Crystal Growth and Characterization of Materials*, 64(3), 75-101.
12. Akan, A. E., & Ünal, F. (2020). Thin-Layer Drying Modeling in the Hot Oil-Heated Stenter. *International Journal of Thermophysics*, 41(8), 1-27.
13. Carrera, E., & Pagani, A. (2014). Free vibration analysis of civil engineering structures by component-wise models. *Journal of Sound and Vibration*, 333(19), 4597-4620.
14. Yilmaz, H. M., Aktan, N., Çolak, A., & Alptekin, A. (2022). Modelling Ozancık village (Aksaray) in computer environment using UAV photogrammetry. *Mersin Photogrammetry Journal*, 4(1), 32-36.
15. Kip, M., & Goren, A. (2022). Güneş Enerjili Hafif Aracın Arka Salıncak Kolunun Topoloji Optimizasyonu Çalışması. *Journal of Science, Technology and Engineering Research*, 3(2), 42-49.
16. Beyazit, N. I., Unal, F., & Bulut, H. (2020). Modeling of the hourly horizontal solar diffuse radiation in Sanliurfa, Turkey. *Thermal Science*, 24(2 Part A), 939-950.
17. Song, J. H. (2015). Pairing effect and tensile properties of laminated high-performance hybrid composites prepared using carbon/glass and carbon/aramid fibers. *Composites Part B: Engineering*, 79, 61-66.
18. Jaroslaw, B., Barbara, S., & Patryk, J. (2016). The comparison of low-velocity impact resistance of aluminum/carbon and glass fiber metal laminates. *Polymer Composites*, 37(4), 1056-1063.
19. Wagih, A., Sebaey, T. A., Yudhanto, A., & Lubineau, G. (2020). Post-impact flexural behavior of carbon-aramid/epoxy hybrid composites. *Composite Structures*, 239, 112022.
20. Gemi, D. S., Şahin, Ö. S., & Gemi, L. (2021). Experimental investigation of the effect of diameter upon low velocity impact response of glass fiber reinforced composite pipes. *Composite Structures*, 275, 114428.
21. Rezasefat, M., Gonzalez-Jimenez, A., Ma, D., Vescovini, A., Lomazzi, L., da Silva, A. A., ... & Manes, A. (2022). Experimental study on the low-velocity impact response of inter-ply S2-glass/aramid woven fabric hybrid laminates. *Thin-Walled Structures*, 177, 109458.
22. Uyaner, M., Kara, M., Kepir, Y., & Gunoz, A. (2022). Virtual Testing of Laminated Composites Subjected to Low-Velocity Impact. *Iranian Journal of Science and Technology, Transactions of Mechanical Engineering*, 1-16.
23. Berk, B., Karakuzu, R., Murat Icten, B., Arikan, V., Arman, Y., Atas, C., & Goren, A. (2016). An experimental and numerical investigation on low velocity impact behavior of composite plates. *Journal of Composite Materials*, 50(25), 3551-3559.
24. Maghsoudlou, M. A., Barbaz Isfahani, R., Saber-Samandari, S., & Sadighi, M. (2021). The response of GFRP nanocomposites reinforced with functionalized SWCNT under low velocity impact: experimental and LS-DYNA simulation investigations. *Iranian Journal of Materials Science and Engineering*, 18(2), 1-11.
25. Sayer, M. (2009). Hibrit kompozitlerin darbe davranışlarının incelenmesi. (PHD Thesis), Pamukkale University.
26. Alkhatib, F., Mahdi, E., & Dean, A. (2020). Crushing response of CFRP and KFRP composite corrugated tubes to quasi-static slipping axial loading:

- experimental investigation and numerical simulation. *Composite Structures*, 246, 112370.
27. Singh, N. K., & Singh, K. K. (2015). Review on impact analysis of FRP composites validated by LS-DYNA. *Polymer Composites*, 36(10), 1786-1798.
28. Uyaner, M., & Kara, M. (2007). Dynamic response of laminated composites subjected to low-velocity impact. *Journal of Composite materials*, 41(24), 2877-2896.



© Author(s) 2023. This work is distributed under <https://creativecommons.org/licenses/by-sa/4.0/>